75th International Astronautical Congress (IAC), Milan, Italy, 14-18 October 2024.

IAC-24,C1,IPB,36,x91025

Autonomous Fault Management in Attitude Determination and Control Subsystems: Hardware and Processor In the Loop Testing

Andrea Colagrossi[a], Andrea Brandonisio[a], Michèle Lavagna[a]

[a] *Politecnico di Milano, Department of Aerospace Science and Technology, Milan, 20156, Italy*

Abstract

An autonomous fault management architecture seamlessly integrated with the Attitude Determination and Control Subsystem (ADCS) brings enhanced reliability and robustness to satellites. Optimized for processors with limited resources, this system detects and isolates hardware failures in real-time, ensuring uninterrupted control by swiftly switching to redundant components or alternative software. By autonomously recalibrating after failures, it guarantees mission continuity even under multiple anomalies. Validated through real-time testing, this approach proves its resilience and reliability, offering a holistic solution for fault tolerance in critical spacecraft operations.

Keywords: fault management; failure detection, isolation and recovery (FDIR), attitude determination and control (ADCS), real-time testing, hardware facility

1. Introduction

The small satellite sector has experienced significant growth in recent years, driven by increasing demand for versatile platforms ranging from microsatellites to nanosatellites [1]. These small systems, although constrained by their size, weight, and complexity, are now technologically mature and play a pivotal role in sophisticated space missions, including large constellations, in-orbit inspections, and distributed sensing. Historically valued for their cost-effectiveness, small satellites have evolved to meet complex mission requirements and must now adhere to quality and reliability standards similar to those of larger spacecraft. However, the size limitations of these platforms pose unique challenges, especially when it comes to their Attitude Determination and Control Subsystem (ADCS), which is responsible for stabilizing and maneuvering the spacecraft.

Despite the maturity of small satellite technology, the ADCS remains a subsystem that frequently contributes to failures, accounting for nearly 18% of mission losses within the first 30 days [2]. This high failure rate emphasizes the need for more reliable and fault-tolerant ADCS solutions. Unlike traditional spacecraft, which may have the luxury of greater redundancy and more robust hardware, small satellites must achieve complex maneuvering and high-precision control within tight constraints on mass, volume, and computational resources. The growing complexity of these control systems has outpaced many of the conventional methods used to ensure spacecraft stability and reliability.

To address these challenges, this paper introduces an autonomous fault-tolerant Attitude Determination and Control Subsystem (ADCS) designed specifically for small satellite platforms [4, 6]. The system integrates fault management functions to ensure continuous and reliable operations, even in the presence of hardware anomalies. By embedding failure detection, isolation, and recovery (FDIR) mechanisms within the ADCS, the proposed architecture not only enhances reliability but also improves the robustness of small satellites to handle failures autonomously. The architecture detects a wide range of anomalies—such as sensor spikes, erratic data trends, hardware malfunctions, thermal issues, and power anomalies—using low computational resources. Once a fault is detected, the system quickly isolates the problematic component, triggering an autonomous reconfiguration that either activates redundant hardware or switches to alternative software processes to maintain control. This ensures uninterrupted satellite operations and minimizes the risk of mission failure. The fault management system is designed to operate in parallel with the core ADCS tasks, ensuring that there are no delays or interruptions in satellite pointing control. Moreover, the architecture autonomously recalibrates and reconfigures after a failure, enabling the spacecraft to continue its mission even with multiple failures. By offering multiple software alternatives and redundant hardware components, the system can adapt to different failure scenarios and transition to a simplified control mode if necessary. In addition to fault detection and isolation, the system incorporates a multi-mode approach that enhances its fault-tolerant capabilities. The attitude determination section consists of independent modes, including full attitude determination, Sun direction estimation, and angular velocity estimation, which ensure accurate determination of the spacecraft's orientation. The system also includes an inertial navigation section

integrated with global navigation satellite system (GNSS) data for orbit determination.

The proposed ADCS architecture provides a holistic solution to the challenges faced by modern small satellite platforms. With its multi-mode, fault-tolerant design, the system delivers the required control and estimation performance while maintaining computational efficiency. It is capable of achieving degree-level attitude accuracy and meter-level position estimation using low-cost, resource-constrained hardware commonly found in small satellite systems. The effectiveness of the proposed system is validated through real-time flat-sat testing [3, 5], which simulates realistic operational conditions with real sensor and actuator telemetry. These tests demonstrate that the system can reliably handle a range of hardware failures while continuing to meet stringent mission requirements. By autonomously managing failures and ensuring continuous spacecraft control, the proposed architecture significantly improves the reliability and robustness of small satellite missions, enabling them to perform complex maneuvers and achieve mission-critical objectives with high accuracy and minimal resource consumption.

2. Autonomous Fault Management Architecture

The system architecture for Autonomous Fault Management in Attitude Determination and Control Subsystems (ADCS) is designed to ensure robust and continuous operation in the event of hardware failures or anomalies. The architecture is divided into several key components: sensor and actuator interfaces, fault detection and isolation (FDI) mechanisms, failure recovery processes, and control algorithms. Sensor and actuator data are continuously monitored and processed in real-time to detect potential anomalies such as sensor drifts, erratic trends, or power fluctuations. Once an anomaly is identified, the fault detection and isolation system pinpoints the malfunctioning component and isolates it from the main ADCS processing chain to prevent further degradation of the system. A recovery routine is then initiated, either activating redundant hardware or switching to software-based alternatives for essential ADCS functions. This entire process operates in parallel with the core ADCS control tasks, ensuring that mission-critical operations such as attitude determination and orbit control are not interrupted. The architecture is designed to handle a wide range of failure modes autonomously, recalibrating and reconfiguring the system as needed to maintain spacecraft stability and control, while minimizing false positives in fault detection. The fault management system also adapts dynamically to mission conditions, switching between operational modes to ensure that the spacecraft can continue to perform its objectives even in degraded states.

The system-level failure detection and isolation block is integrated with reconfiguration logic in the ADCS manager, enabling autonomous recovery in the event of non-nominal scenarios. These blocks continuously gather status information from various aspects of the ADCS, including the current nominal operational mode, sensor health, and the error status of attitude and orbit determination functions. When a combination of these parameters indicates an abnormal or incompatible status, the failure detection monitor raises an error flag. At this point, specialized isolation algorithms are triggered to confirm the failure and evaluate potential redundant configurations. These algorithms take into account previous failures, attempt to reboot malfunctioning components, and assess the availability of redundant hardware or software alternatives. Based on the outcome of this analysis, the ADCS manager dynamically reconfigures the system to ensure continued functionality in line with the platform's operational mode. For example, it may activate backup sensors or switch to alternative attitude determination algorithms to maintain required system outputs. If redundancy options are exhausted or the system cannot meet performance requirements, the ADCS manager initiates a transition to a platform safe mode, ensuring the satellite's stability and initiating a mode switch to a compatible configuration that can continue to operate under the degraded conditions.

An example architectural implementation of the proposed system, for a pair of attitude and orbit determination functions, is reported in Figure 1.

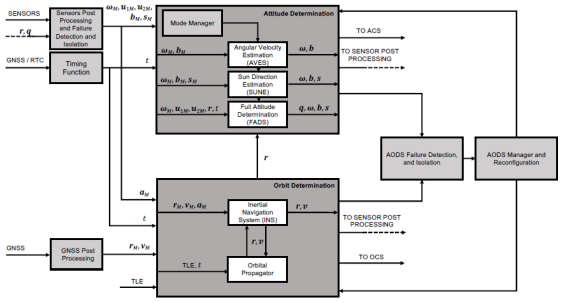

Figure 1: Example Architectural Implementation of an Autonomous Fault Management System

2.1 Component Level Failure Detection and Isolation

At the component level, failure detection and isolation functions operate on the sensor signals after they have undergone low-pass filtering. This approach ensures that failure detection is performed on the raw, filtered sensor

measurements, using statistical analysis to identify anomalies in the incoming signal. The filtering process is standardized across sensors, regardless of whether or not they have built-in low-pass filtering.

The statistical algorithms used are calibrated to detect the most common types of sensor faults, which include spike faults, erratic faults, drift faults, hardover/bias faults, data loss faults, and stuck faults. These faults are categorized as follows:

- **Spike Faul**t: Sudden spikes appear in the sensor output.
- **Erratic Fault**: A significant increase in noise is observed in the sensor output.
- **Drift Fault**: The sensor output consistently increases or decreases from its nominal state.
- **Hardover/Bias Fault:** A sudden, sustained shift in the sensor output occurs.
- **Data Loss Faul**t: There are time gaps where no data is available.
- **Stuck Fault**: The sensor output becomes fixed at a single value.

Detecting these faults is challenging due to the dynamic nature of the nominal sensor signals, which vary with the spacecraft's attitude. For instance, none of the sensor outputs remain constant in a steady state, so the detection algorithms must differentiate between nominal sensor variations and faulty ones. Since spacecraft rotations are limited by maximum angular rates and accelerations by the actuator torques, there is a maximum feasible time variation in sensor signals that helps distinguish between realistic measurements and faulty signals.

The algorithms minimize the risk of marking valid signals as faulty through system-level failure detection, which compares multiple measurements to identify dangerous conditions. However, the approach is intentionally conservative to prevent fault propagation. It is preferable to detect false failures rather than allow an undetected failure to impact the Attitude Determination and Control Subsystem (ADCS).

Failure detection is based on the running variance and mean of sensor signals. The running variance detects common sensor faults, while the running mean is used to check if a valid sensor output is present. If sensor data are missing or corrupted, the sensor driver sets the measurements to zero. For the *j*-th sensor measurement, the running variance and mean over the last S samples are computed as follows:

$$\sigma_j(t_S) = \frac{1}{S}\sum_{i=1}^{S} u_j^2(t_{S+1-i}) - \left(\frac{1}{S}\sum_{i=1}^{S} u_j(t_{S+1-i})\right)^2$$

$$\mu_j(t_S) = \frac{1}{S}\sum_{i=1}^{S} u_j(t_{S+1-i})$$

For sensors measuring vector quantities, the running variance and mean are calculated for each component of the vector:

$$\sigma_j(t_S) = \left[\sigma_{j_1}(t_S), \sigma_{j_2}(t_S), \sigma_{j_3}(t_S)\right],$$

$$\mu_j(t_S) = \left[\mu_{j_1}(t_S), \mu_{j_2}(t_S), \mu_{j_3}(t_S)\right]$$

A sensor is considered functional if the running mean of the variance is greater than zero and below a threshold. For vector sensors, the minimum running mean of the variance components must be greater than zero, and the maximum component must be below the threshold:

$$\min\left(\frac{1}{S}\sum_{i=1}^{S} \sigma_j(t_{S+1-i})\right) > 0$$

$$\text{and} \quad \max\left(\frac{1}{S}\sum_{i=1}^{S} \sigma_j(t_{S+1-i})\right) < \tau_j$$

If these conditions are not met, the sensor is considered faulty. For stuck faults, the minimum component is zero, while a high variance suggests other faults like erratic or spike faults. The variance threshold \(\tau_j \) is sensor-specific and calibrated through ground testing, and its value can be updated in orbit to adjust the failure detection sensitivity.

A sensor is operational if the square of the running mean, or the square of the minimum running mean component for vector signals, is greater than zero:

$$\min\left(\mu_j^2(t_S)\right) > 0$$

If this condition is not met for an extended period, the sensor is considered off. Short and intermittent failures may indicate data loss faults.

If a failure is detected based on either of the above conditions, the faulty sensor is isolated, as reported in the examples in Figures 2 and 3. The system attempts to reboot the sensor and, if it fails again, the sensor is deactivated.

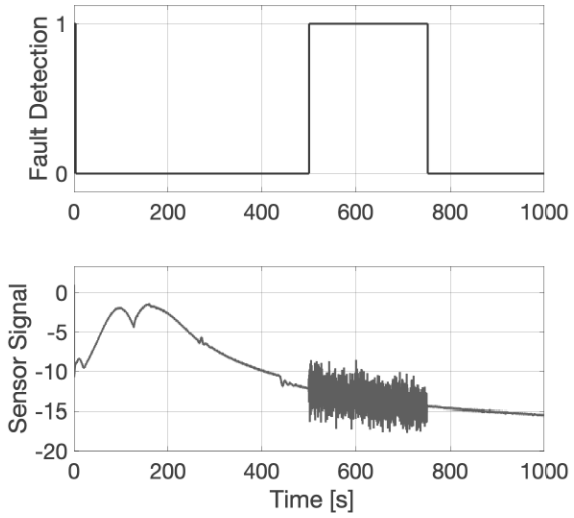

Figure 2: Example Fault Detection on an Erratic Sensor Measurement.

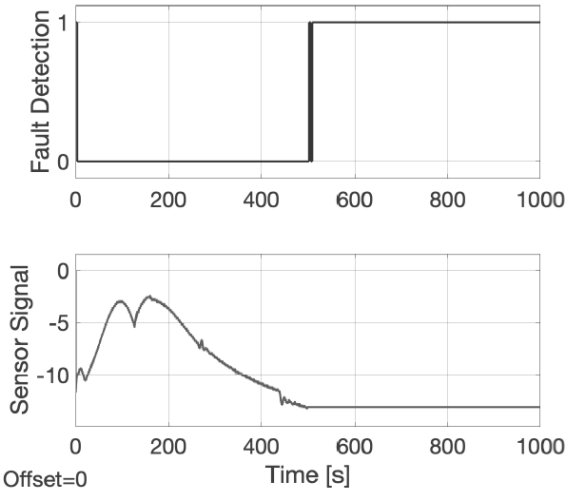

Figure 3: Example Fault Detection on a Stuck Sensor.

2.2 Redundant Component Management

Redundant components are managed by a dedicated function that processes inputs from the ADCS manager, failure detection and isolation (FDI) algorithms, and the corrected sensor signals.

When a sensor failure is detected, the affected component is excluded from further ADCS operations. Until the isolation functions or ground commands confirm the sensor's recovery, its data are blocked. If no redundant sensor is available after a failure, the system-level FDI detects this, prompting the ADCS manager to reconfigure the system to meet operational requirements. If this is not feasible, a safe mode is initiated, or a critical ADCS error is reported to the platform.

The ADCS manager selects and commands the most appropriate sensors and estimation algorithms based on the current configuration. For instance, if angular velocity estimation is required, the system provides the necessary angular velocity and magnetic field measurements. If reconfiguration is necessary, the manager chooses an alternative set of sensors to maintain functionality.

When multiple redundant sensors are available, the system selects the one with the lowest variance, as higher variance indicates greater measurement errors. The selected sensor is given by:

$$\breve{u} = u_k,$$

where

$$\frac{1}{S}\sum_{i=1}^{S}\sigma_k(t_{S+1-i}) < \frac{1}{S}\sum_{i=1}^{S}\sigma_j(t_{S+1-i}) \quad \forall j \neq k$$

In cases where the quality of sensors differs significantly, only the most accurate available sensor is used, with coarse sensors activated only if necessary. If needed, failure thresholds for accurate sensors are set below the typical variance of coarse sensors. In Figure 4, the used sensor is Sensor 1 at the beginning, then a spike in its measurements at t = 50 make the system to transition to Sensor 2. However, when Sensor 2 fails at t = 500, the used measurement is back again to use Sensor 1. Note how Sensor 1 and Sensor 2 are characterized by different bias values.

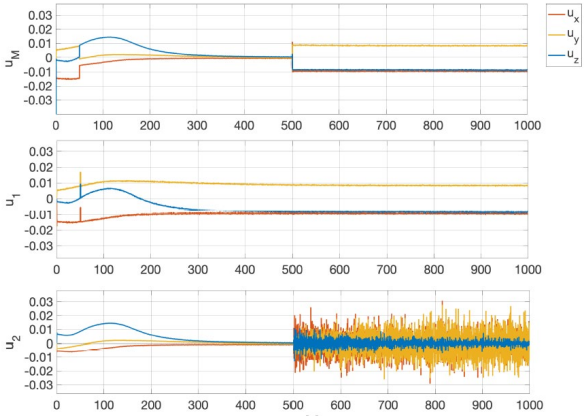

Figure 4: Example Redundant Component Selection

3. Real-time Testing Facility

To ensure the reliability and robustness of the proposed Autonomous Fault Management system for the Attitude

Determination and Control Subsystem (ADCS), comprehensive testing and validation are essential. This process involves the use of advanced simulation tools combined with real-time hardware integration. Specifically, a Hardware-in-the-Loop (HIL) and Processor-in-the-Loop (PIL) testing facility will be employed to rigorously evaluate the performance of the system under various fault conditions and operational scenarios.

The HIL and PIL methodologies provide a critical link between theoretical models and real-world application by allowing the proposed algorithms and control strategies to be tested in an environment that mimics the actual spacecraft dynamics. These facilities integrate real-time processing units and flight-equivalent hardware with high-fidelity software simulations, ensuring that the fault management system operates as intended under realistic conditions. The ability to simulate sensor behavior, faults, and actuator responses in real-time allows for thorough validation, covering both nominal and non-nominal scenarios.

By leveraging this real-time setup, the proposed system's fault detection, isolation, and recovery mechanisms can be rigorously validated, with any performance gaps identified and corrected before deployment on an actual spacecraft. This section will detail the design of the HIL and PIL facilities, describe the test scenarios employed, and present the results of these validation activities.

The developed real time flat-sat facility for testing is designed to replicate the spacecraft's dynamic behavior, external environment, and the interactions between ADCS peripherals through a digital twin model. This enables the testing and validation of the proposed system without the need for costly and complex physical motion platforms. The core of this facility is built to ensure reliable and repeatable testing outcomes, fulfilling several key requirements:

- Update rate ranging from 1 Hz to 10 Hz for dynamics simulations.
- Sensor/actuator sampling at frequencies over 10 Hz, mirroring the real hardware.
- Measurable real-time performance ensuring minimal timing delays and system responsiveness.
- Robust data exchange without corruption or loss during testing.
- Support for standard communication interfaces, including UART, SPI, I2C, and CAN.
- Analog-to-digital conversion and signal sampling for sensor emulation.

Given its emphasis on small satellite applications, this testing facility is designed to be budget-conscious and easy to implement. The development process balances functionality with practicality, taking into account the constraints of time, budget, and the medium-level engineering skills typically available in small satellite projects. By following this CubeSat-oriented approach, the facility can be tailored to meet the requirements of various ADCS validation scenarios, significantly contributing to the reliability of nanosatellite missions.

The final design of the facility relies on hardware interface boards for data exchange between the simulation computer, which runs the dynamic and environmental simulation, and the on-board computer (OBC) under testing. These boards consist of single-board microcontrollers that simulate the behavior of ADCS peripherals, processing numerical sensor data from the digital twin model and transmitting it to the OBC via standard spacecraft communication protocols. This setup mimics the speed, commands, data formats, and error checks of real sensors, allowing the OBC to interact with simulated peripherals as though they were actual hardware components.

The simulation computer, equipped with the Simulink Desktop Real-Time (SDRT) framework, handles the real-time dynamics and environmental simulation. Operating on a standard Windows or macOS workstation, the SDRT framework allows simulations to run at performance levels up to 20 kHz. It ensures precise synchronization between the simulation and the hardware, and monitors for any potential real-time performance losses, making it possible to identify and discard tests that do not meet timing requirements.

Simulink is used to develop the dynamic and environmental simulators according to the European Cooperation for Space Standardization (ECSS) guidelines. The simulators accurately recreate sensor outputs based on component specifications or physical performance data, enabling high-fidelity emulation of real-world ADCS operations. Figure 5 reports a schematic diagram of the developed facility.

The interface boards between the simulation computer and the OBC replicate the electrical and data interfaces of the spacecraft's ADCS peripherals. These microcontroller boards emulate the communication protocols (e.g., UART, I2C, SPI) between the OBC and the sensors/actuators, allowing the OBC to perceive the simulated sensor data as if it were real. The boards are modular, easily programmable, and capable of replicating the full functionality of individual sensors or groups of sensors.

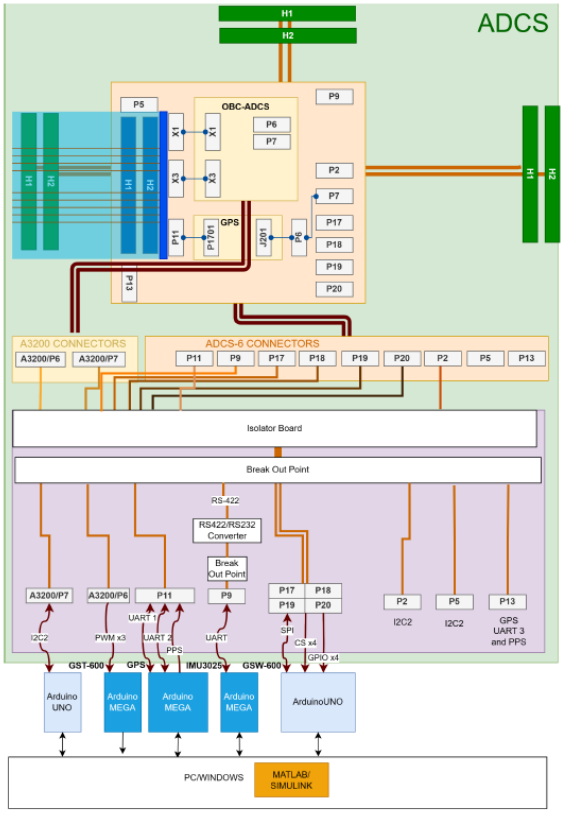

Figure 5: Real-time Testing Facility Scheme

1. *UART*: The facility supports UART-based communications, including standards like RS-232 and RS-485, by simulating the peripheral behavior through serial data exchange between the simulation computer and the OBC. The UART communication replicates the physical sensor measurements in the exact format, including message headers and checksums.

2. *I2C*: The I2C interface allows the facility to simulate multiple sensors through a single microcontroller board by using a multi-slave design. The microcontroller responds to master device calls for multiple I2C addresses, allowing it to simulate multiple instruments as part of the ADCS architecture.

3. *SPI*: SPI communication is implemented for actuators or devices requiring high-speed, synchronous serial communication. The microcontroller's GPIO pins are used to handle multiple slaves through individual chip select lines, simulating realistic peripheral behavior in the spacecraft.

4. *Analog and Digital Interfaces*: The facility can also handle analog-to-digital data conversion and replicate modulated signals like Pulse-Width Modulation (PWM), ensuring that the system can validate a wide range of sensor and actuator types.

3.1 System Flexibility and Scalability

The facility's modular architecture is a key feature that allows it to adapt to different test scenarios. Using COTS microcontrollers with C-based programming, the facility is flexible and scalable, able to handle different digital communication protocols and even replicate custom data exchanges used by specific flight software. By configuring each microcontroller to simulate a finite state machine (FSM) of a peripheral, the facility can be tailored to replicate various operational modes and communication patterns used in nanosatellite ADCS systems.

The primary communication link between the simulation computer and the microcontrollers is via USB, while the link between the microcontrollers and the OBC replicates the spacecraft's actual electrical interfaces. To ensure safety during testing, the facility includes galvanic isolation between the OBC and the microcontrollers, protecting the hardware under test from electrical damage.

Through the use of SDRT, the simulation computer maintains real-time synchronization with the testing hardware, ensuring that any performance deviations (e.g., missed ticks) are detected and logged. This real-time monitoring capability ensures that the facility operates within defined performance parameters, making it highly suitable for testing ADCS systems that require precise timing and synchronization, as is often the case in small satellite missions.

With its flexible and cost-effective design, the developed real-time testing facility provides a robust platform for validating ADCS systems, helping ensure mission success for nanosatellites.

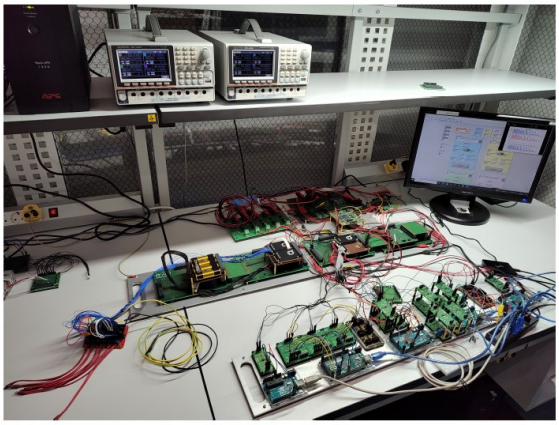

Figure 6: Real-time Testing Facility Overview

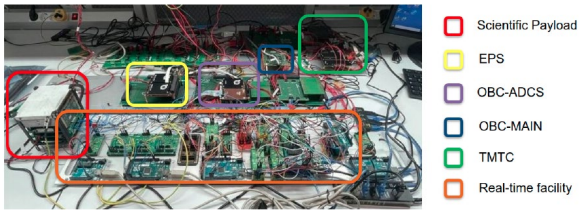

Figure 7: Real-time Testing Facility for HERMES System Testing [7, 21, 22].

4. Testing Results

The previously described real time testing facility was designed to emulate with on-board processor and hardware in the loop the behavior of the ADCS system in a high-fidelity environment, allowing for rigorous validation of the system's performance. This section presents the results of testing the developed autonomous fault management system using real-time simulation and integration with the actual On-Board Computer (OBC). The goal of these tests was to validate the end-to-end functionality, communication interfaces, and real-time performance of the ADCS subsystems under varying conditions.

Key performance metrics, including sensor data accuracy, actuator command response, and communication reliability, were assessed under operational constraints. The testing campaign focused on evaluating the system's ability to maintain synchronization between the simulated dynamics and the physical hardware, ensuring that the PIL setup could effectively replicate real-world conditions.

By employing a modular test setup, various ADCS scenarios were replicated, allowing for comprehensive assessment of system behavior in different mission profiles. The results outlined in this section provide insights into the system's robustness, highlighting both the strengths and areas for potential refinement, ultimately contributing to the development of a more reliable and efficient ADCS for small spacecraft missions.

The proposed fault management system ensures continuous operation, even in the presence of multiple faults. While the estimation performance degrades under these conditions, the system is still capable of providing state estimation. The redundant sensor management system immediately switches between redundant components, preventing fault propagation within the determination system.

Figure 8 illustrates the system capabilities mode during a Sun-pointing operation, where multiple failures were injected into the real-time testing facility. The system under evaluation is equipped with fine Sun sensors, two gyroscopes of similar accuracy, and two magnetometers with differing performance levels. The redundant magnetometer exhibits significant bias and noise compared to the primary one.

The simulated failures include: the loss of the primary gyroscope at approximately 2000 seconds, the loss of both gyroscopes at around 4000 seconds, the loss of the primary magnetometer at approximately 11,000 seconds (after the gyroscopes were restored at around 10,000 seconds), and the loss of Sun sensors at around 18,000 seconds.

The system begins with an unknown attitude state and takes approximately 500 seconds to complete its initial calibration and achieve accurate attitude estimation. During this phase, the dynamics are not yet controlled, and Sun acquisition and pointing only begin after a delay. The first eclipse starts with a rough estimate of the gyroscope bias, followed by the failure of the primary gyroscope, causing propagation errors to increase beyond 50 degrees. Correct attitude estimation is restored once the Sun data become available after the eclipse. Subsequently, both gyroscopes fail, and the system switches to angular rate estimation using magnetometers. This reconfiguration is evident in the system output, where a large instantaneous error occurs at around 4000 seconds, followed by a correct, albeit noisier, attitude estimation due to the numerical derivatives required to compute angular rates from magnetic measurements. The error does not propagate into the control blocks, as it is contained during the AODS manager's reconfiguration process.

The gyroscope fault is recovered around 10,000 seconds, just after the second eclipse period. At approximately 11,000 seconds, the primary magnetometer fails, and the large bias of the secondary magnetometer introduces significant attitude determination errors, which are reduced during the recalibration process. However, the high noise level of the redundant magnetometer prevents fine calibration, resulting in a steady-state attitude error higher than in the nominal case. The third dead reckoning period ends around 15,000 seconds, with an estimation error of around 10 degrees. Finally, at approximately 18,000 seconds, the Sun sensors fail, and the system reverts to angular rate estimation, with attitude errors oscillating between 10 and 20 degrees.

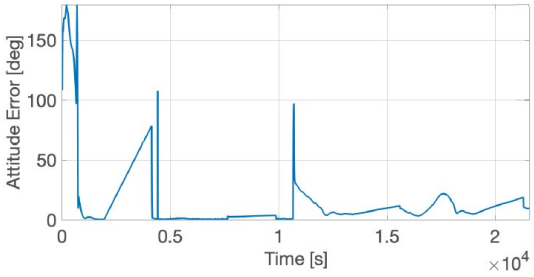

Figure 8: Attitude State Estimation with Multiple Failures (Gyroscopes loss at 4000 s. Primary magnetometer loss at 11,000 s. Sun sensors loss at 18,000 s .)

In an analogous case, applied to an ADCS for flexible spacecraft control [20], where complete system errors were not injected, the fault management system oversees switch between redundant sensors and control on-board calibration. In this case, the attitude determination error remained below 3 degrees throughout the entire period, as shown in Figure 9, with the exception of a brief peak at approximately 17,000 seconds and a gradual increase in error between 2000 and 4000 seconds. The peak at around 17,000 seconds was a minor fluctuation in the determination functions, similar to others typically observed during the attitude estimation process. These small spikes in the attitude determination error often occur when switching between fine Sun sensors with the Sun near the edge of the sensor's field of view, particularly during yaw rotations. Such peaks would not be present if the attitude determination were conducted in inertial attitude mode.

The initial rise in attitude determination error was associated with the first dead-reckoning period during the initial eclipse, when the gyroscope biases were not yet fully estimated. Consequently, the attitude determination system was not fully calibrated during the first orbit. This issue can be partially mitigated by initializing the calibration functions with ground-estimated biases, although the launch event is likely to disrupt these calibration values. Nonetheless, when the biases were correctly estimated on-board, the dead-reckoning attitude propagation did not exceed the 3-degree error threshold. This is evident in Figure 9 during the subsequent three eclipse periods at approximately 9000 seconds, 14,000 seconds, and 20,000 seconds.

The sensor calibration significantly enhanced the full-attitude determination functions, improving estimation accuracy both during sunlight and eclipse phases. The onboard autonomous calibration system continuously operates to correct sensor drift and recalibrate the entire system if a primary sensor fails and a redundant one is activated. This effectiveness is attributed to the relatively rapid dynamics of the calibration algorithms.

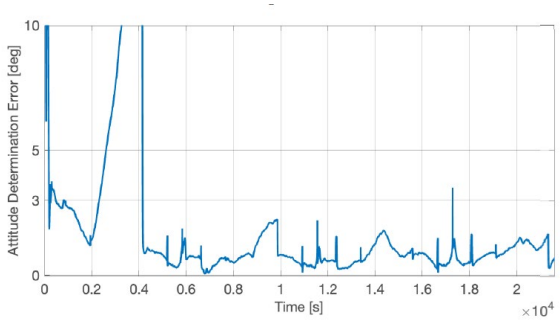

Figure 9: Attitude State Estimation in Zenith Pointing Mode.

Figures 10 and 11 illustrate the residual error in the calibrated angular velocities and magnetic field, respectively. In both cases, the calibration functions, starting from initial zero conditions, succeeded in eliminating measurement errors within 30 minutes. This allowed for a complete system calibration within a single orbital period, which is crucial for spacecraft operations and managing error drifts. Additionally, it was observed that the initial cold start trend, which typically causes slower convergence of calibration filters, did not affect the attitude determination functions once they were fully operational.

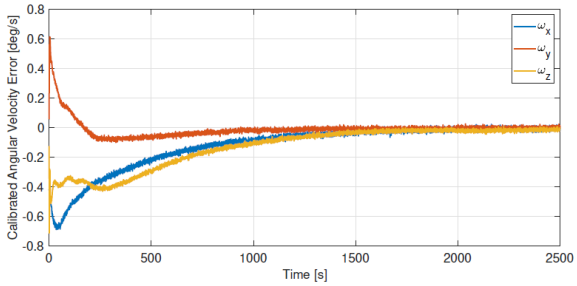

Figure 10: Angular Velocity Calibration Error.

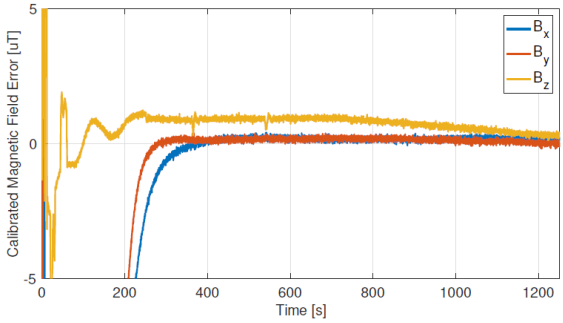

Figure 11: Magnetic Field Calibration Error.

The overall ADCS pointing performance, with autonomous sensor calibration and redundant sensor management undergoing in the loop, with single failure injection, as in the case reported in Figure 9, have been tested in real time, proving the positive ADCS

performance over a period of 1 day in orbit. The result in reported in Figure 12, where, after the initial 1h of system calibration and correct state estimation, the system maintains an average pointing error lower than 5 degrees.

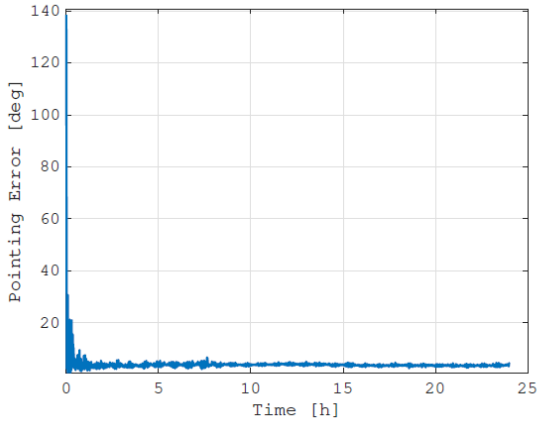

Figure 12: Pointing Error in Zenith Pointing Mode.

5. Conclusion

The proposed full Attitude Determination and Control System (ADCS) incorporating an autonomous fault management system demonstrates its robust performance under various fault conditions. The ADCS effectively maintains attitude estimation capabilities even when multiple sensor failures occur. Although estimation accuracy is affected, the proposed architecture ensures continued operation by managing redundant sensors and preventing the propagation of faults into the determination and control functions. This capability is crucial for maintaining reliable satellite operations despite encountering sensor malfunctions.

The results from the Hardware-in-the-Loop (HIL) testing, as detailed in the provided results, confirm the efficacy of the proposed ADCS in handling diverse failure scenarios. For instance, the testing revealed that the attitude determination error remained below 3 degrees throughout most of the operation, with minor deviations attributable to transient peaks and calibration-related errors. The system demonstrated resilience by recalibrating and adapting to changing conditions, maintaining performance within acceptable limits. Indeed, the overall pointing performance is never affected above 5 degrees, except for the initial state acquisition and calibration time.

The autonomous calibration feature of the system further enhances its reliability by continuously adjusting for sensor drift and recalibrating the system when necessary. This self-correcting capability is critical for minimizing errors and ensuring accurate attitude determination and control both in sunlight and during eclipses. The calibration functions, initialized from zero, proved effective in reducing measurement errors within 30 minutes, achieving complete system calibration within an orbital period. This rapid convergence underscores the system's adaptability and efficiency in real-time operations.

In summary, the proposed autonomous fault management system not only meets the requirements for reliable attitude control under fault conditions, but also benefits from efficient autonomous calibration. The system's performance, validated through rigorous real time testing, highlights its suitability for small satellite platforms, ensuring robust and accurate attitude control in various operational scenarios.

References

[1] Raghunath, K.; Kang, J.S. An Exploration of the Small Satellite Value Chain and the Future of Space Access. In Proceedings of the AIAA/USU Conference on Small Satellites: Mission Operations & Autonomy, Virtual, 7–12 August 2021; Number SSC21-P1-29.

[2] Perumal, R.P.; Voos, H.; Vedova, F.D.; Moser, H., Small Satellite Reliability: A Decade in Review. In Proceedings of the AIAA/USU Conference on Small Satellites: Mission Operations & Autonomy, Virtual, 7–12 August 2021; Number SSC21-WKIII-02.

[3] Silvestrini, S.; Colagrossi, A.; Lavagna, M.; A Flat-Sat Platform for the Development and Testing of the 3U Hermes Constellation Satellites, In Proceedings of the 74th IAC 2023, Baku, Azerbaijan, 2–6 October 2023.

[4] Colagrossi, A.; Brandonisio, A.; Capra, L.; Silvestrini, S.; Lavagna, M.; Hermes ADCS: From System Design to Pre-Flight Verification and Testing, In Proceedings of the 74th IAC 2023, Baku, Azerbaijan, 2–6 October 2023.

[5] Colagrossi, A.; Silvestrini, S.; Lavagna, M.; Flat-Sat Facility for Processor-in-the-Loop Verification and Testing of Nanosatellite ADCS, In Proceedings of the ESA GNC 2023, Sopot, Poland, 12–16 June 2023.

[6] Colagrossi, A.; Prinetto, J.; Silvestrini, S.; Orfano, M.; Lavagna, M.; Fiore, F.; Burderi, L.; Bertacin, R.; Pirrotta, S. Semi-analytical Approach to Fasten Complex and Flexible Pointing Strategies Definition for Nanosatellite Clusters: The HERMES Mission Case from Design to Flight. In Proceedings of the 70th International Astronautical Congress (IAC 2019), Washington, DC, USA, 21–25 October 2019; pp. 1–8.

[7] Colagrossi, A.; Silvestrini, S.; Prinetto, J.; Lavagna, M. HERMES: A CubeSat-Based Constellation for the New Generation of Multi-Messenger Astrophysics. In Proceedings of the 2020 AAS/AIAA Astrodynamics Specialist Conference, Lake Tahoe, CA, USA, 9–12 August 2020; pp. 1–20.

[8] Markley, F. Attitude Determination Using Two Vector Measurements; Number NASA/CP-1999-209235; NASA Flight Mechanics Symposium: Washington, DC, USA, 1999; pp. 39–52.

[9] Springmann, J.C.; Sloboda, A.J.; Klesh, A.T.; Bennett, M.W.; Cutler, J.W. The Attitude Determination System of the RAX Satellite. Acta Astronaut. 2012, 75, 120–135.

[10] Schmidt, M.; Ravandoor, K.; Kurz, O.; Busch, S.; Schilling, K. Attitude Determination for the Pico-Satellite UWE-2. IFAC Proc. Vol. 2008, 41, 14036–14041.

[11] Makovec, K.L.; Turner, A.J.; Hall, C.D. Design and Implementation of a Nanosatellite Attitude Determination and Control System. In Proceedings of the 2001 AAS/AIAA Astrodynamics Specialists Conference, Quebec City, QC, Canada, 30 July–2 August 2001; Number AAS 01-311.

[12] Mahony, R.; Hamel, T.; Pflimlin, J.M. Complementary Filter Design on the Special Orthogonal Group SO(3). In Proceedings of the 44th IEEE Conference on Decision and Control, Seville, Spain, 12–15 December 2005; pp. 1477–1484.

[13] Mahony, R.; Hamel, T.; Pflimlin, J.M. Nonlinear Complementary Filters on the Special Orthogonal Group. IEEE Trans. Autom. Control. 2008, 53, 1203–1218.

[14] Dong, Y. MEMS Inertial Navigation Systems for Aircraft. In MEMS for Automotive and Aerospace Applications; Kraft, M., White, N.M., Eds.; Woodhead Publishing Series in Electronic and Optical Materials; Woodhead Publishing: Sawston, UK, 2013; pp. 177–219.

[15] Wahba, G. A Least Squares Estimate of Satellite Attitude. SIAM Rev. 1966, 7, 409.

[16] Markley, F.L.; Mortari, D. Quaternion Attitude Estimation Using Vector Observations. J. Astronaut. Sci. 2000, 48, 359–380.

[17] Shuster, M.D. The Quest for Better Attitudes. J. Astronaut. Sci. 2006, 54, 657–683.

[18] Alonso, R.; Shuster, M.D. TWOSTEP: A Fast Robust Algorithm for Attitude-Independent Magnetometer-Bias Determination. J. Astronaut. Sci. 2002, 50, 433–451.

[19] Crassidis, J.L.; Lai, K.L.; Harman, R.R. Real-Time Attitude-Independent Three-Axis Magnetometer Calibration. J. Guid. Control. Dyn. 2005, 28, 115–120.

[20] Titterton, D.; Weston, J.L.; Weston, J. Strapdown Inertial Navigation Technology; Institution of Engineering and Technology: London, UK, 2004.

[21] Colagrossi, A, Lavagna, M. Integrated vibration suppression attitude control for flexible spacecrafts with internal liquid sloshing. Multibody Syst. Dyn. 2021, 51-2, 123–157

[21] Burderi, L.; Di Salvo, T., Sanna, A., et al. GrailQuest & HERMES: Hunting for gravitational wave electromagnetic counterparts and probing space-time quantum foam. In Proceedings of SPIE - The International Society for Optical Engineering, Space Telescopes and Instrumentation 2020: Ultraviolet to Gamma Ray, Virtual, Online, 14-18 December 2020, Article number 114444Y.

[22] Sanna, A., Gambino, A. F, Burderi, L, et al. Timing techniques applied to distributed modular high-energy astronomy: The HERMES project. In Proceedings of SPIE - The International Society for Optical Engineering, Space Telescopes and Instrumentation 2020: Ultraviolet to Gamma Ray, Virtual, Online, 14-18 December 2020, Article number 114444X.